Supporting Information

Lee et al. 10.1073/pnas.1212371109

SI Materials and Methods

IgG and Fab Cloning, Expression, and Purification. S139/1 IgG was purified from mouse ascites as previously described (1). S139/1 Fab was cloned into the pFastBac Dual vector (Invitrogen) with N-terminal gp67 signal peptides fused to the light and heavy chains and a C-terminal His_6 tag fused to the heavy chain. Recombinant bacmid DNA was generated using the Bac-to-Bac system (Invitrogen) and baculovirus was generated by transfecting purified bacmid DNA into Sf9 cells using Cellfectin II (Invitrogen). S139/1 Fab protein was expressed by infecting suspension cultures of High Five cells (Invitrogen) with baculovirus at a multiplicity of infection of 5–10 and incubating at 28 °C shaking at 110 rpm for 72 h. The supernatant was harvested by centrifugation at 2,000 × *g* at 4 °C, concentrated, and buffer exchanged into 1× PBS. The Fab was purified by Ni-NTA (Qiagen), protein G, and MonoS chromatography (GE Healthcare). S139/1 has an *N*-glycosylation site at Asn72 in framework region 3 (FR3) of the heavy chain. The Fab separated in three peaks by cation exchange chromatography, which are consistent with unglycosylated, N-linked $Man_3GlcNAc_2Fuc_2$, and possibly a single O-linked GlcNAc or GalNAc (undetermined site) species designated as unglycosylated, glycosylated, and monoglycosylated Fabs, respectively. The identities of each peak were confirmed by mass spectrometry (Table S4). Each peak was pooled separately and purified by a final step of gel filtration (GE Healthcare).

HA Expression and Purification. HA was prepared for binding studies and crystallization as previously described (2). Briefly, each HA (Table 1 and Table S1) was fused with an N-terminal gp67 signal peptide and a C-terminal BirA biotinylation site, thrombin cleavage site, trimerization domain, and a His_6 tag. The HAs were expressed, as described above for the S139/1 Fab, as either mature HA (HA1/HA2) or HA0 and purified by Ni-NTA. Because of the polybasic linker between HA1 and HA2 for certain strains, mature HA was produced and purified. For crystallization, the HA0 of Vic75/H3 was treated with trypsin (New England Biolabs) to remove the C-terminal tags and cleave HA0 to produce mature HA. The trypsin-digested HA was then purified by a final step of gel filtration. For binding studies, each HA0 or mature HA was biotinylated with BirA and purified by gel filtration.

K_d Determination. K_d values were determined by bio-layer interferometry using an Octet RED instrument (ForteBio) as previously described (2). Briefly, biotinylated HAs at ∼10–50 μg/mL in 1× kinetics buffer (1× PBS pH 7.4, 0.01% BSA, and 0.002% Tween 20) were immobilized onto streptavidin-coated biosensors and incubated with varying concentrations of S139/1 Fab or IgG. All binding data were collected at 30 °C. The k_{on} and k_{off} values of Fab and IgG were measured in real-time to determine K_d values for the Fab and IgG for each HA tested. The experimental binding curves of glycosylated and unglycosylated S139/1 Fab and IgG for fitting k_{on} and k_{off} are reported in Figs. S6–S8. The sequences of the HA proteins used in the binding studies are included below.

Plaque Reduction Assays. Neutralization activity of S139/1 Fab and IgG was tested by a plaque reduction assay as previously described (1). The experimental curves are reported in Fig. S9.

Crystallization. Glycosylated S139/1 Fab crystals were grown by sitting drop vapor diffusion at 20 °C by mixing 0.5 μL of concentrated protein sample (∼3.5 mg/mL) with 0.5 μL of mother liquor (2 M ammonium sulfate, 0.1 M sodium citrate pH 5.5) and crystals appeared in 7 d. The Fab crystals were cryoprotected with mother liquor supplemented with 20% (vol/vol) glycerol, flash-cooled, and stored in liquid nitrogen until data collection.

For Fab-HA complex formation, glycosylated S139/1 Fab was added to Vic75/H3 HA in a molar ratio of 3.2:1 to achieve three Fabs per HA trimer and incubated at room temperature for 1 h. The complex was purified from unbound Fab by gel filtration in 50 mM NaCl, 10 mM Tris pH 8.0. S139/1-Vic75/H3 HA crystals were grown by sitting-drop vapor diffusion at 20 °C by mixing 0.5 μL of concentrated protein sample (∼9 mg/mL) with 0.5 μL of mother liquor [2 M ammonium sulfate, 0.1 M Hepes pH 7.5, 2% (vol/vol) PEG 400], and crystals appeared in 7–28 d. The crystals were cryoprotected with mother liquor supplemented with increasing concentrations of glycerol [3% (vol/vol) steps, 5 min per step] to a final concentration of 21% (vol/vol), flash-cooled, and stored in liquid nitrogen until data collection.

Structure Determination and Refinement. Diffraction data were collected on the GM/CA CAT 23-ID-D beamline at the Advanced Photon Source (APS). The glycosylated S139/1 Fab dataset to 2.05 Å was collected and processed in spacegroup $P3_212$ using XDS. The structure was solved by molecular replacement with Phaser (3) using Fab NC-1 (PDB ID code 3OZ9) as the search model and two Fab copies were found in the asymmetric unit. The light chain constant κ-domain from Fab 29G12 (PDB ID code 1MEX), which had higher sequence identity to the S139/1 light variable domain, was then superimposed onto the light chain constant domain of the molecular replacement solution and was used for refinement. This crystal was twinned so the twin law -h, -k, -l, suggested by phenix.xtriage, was applied and R_{free} flags were recalculated during refinement. Rigid body refinement (set for each Ig domain), simulated annealing, and restrained refinement including TLS refinement (set for each Ig domain) were performed using Phenix (4).

The complex dataset to 2.95 Å was collected and processed in spacegroup C2 using XDS. The structure was solved by molecular replacement using an apo A/Hong Kong/1/1968 (H3N2) HA trimer (PDB ID code 4FNK) as the search model and one copy was found in the asymmetric unit. The variable domain of the Fab from above was used as search models and three copies were found that bound around each receptor binding site of the HA trimer. The constant domain was then used as search models and only two of the expected three copies were found. Weak density was observed in the crystal asymmetric unit for the remaining constant domain and it was docked in by hand. Poorly defined regions in the model were trimmed and the complex was run through rigid body refinement (for each Ig domain and HA protomer), simulated annealing, and restrained refinement including TLS refinement (set for each Ig domain and HA protomer) using Phenix. Each model was refined using riding hydrogens generated by phenix.reduce that were then trimmed before PDB deposition.

Structural Analyses. Hydrogen bonds and van der Waals contacts were calculated using HBPLUS and CONTACSYM, respectively (5, 6). Surface area buried upon Fab binding was calculated using MS (7). MacPyMol (DeLano Scientific) was used to render structure figures. Kabat numbering was applied to the coordinate

files using the AbNum server (8). The final coordinates were validated using the JCSG quality control server (v2.8), which includes Molprobity (9).

Sequence Analysis of S139/1 Epitope Conservation. All full-length and nonredundant influenza A HA sequences were downloaded from the Influenza Virus Resource at the National Center for Biotechnology Information (NCBI) database (10). At the time of download (April 11, 2012), the dataset included 13,627 sequences encompassing all 17 influenza A subtypes. The sequences were aligned using MUSCLE (11) and analyzed using GCG (Accelrys) and custom shell scripts (available from the authors upon request).

We assessed the recognition potential of S139/1 to other HA strains by analyzing the sequences from all deposited strains from the Influenza Virus Resource at the NCBI database. We first filtered strains by eliminating those that do not contain the 130-loop and the 150-loop insertions. None of the strains from the H2 and H3 subtypes contain insertions at these loops and so the sequences were further inspected. Of the H2 strains, 89% (178 of 200 sequences) have the essential Lys156 and Gly158 residues. Among these, the 193 position is >98% Ala or Thr, which would not sterically occlude S139/1 binding.

In contrast, only ~20% of H3 strains (591 of 3,033 sequences) appear to be susceptible to S139/1 recognition. These H3 strains are heavily represented in viruses isolated from zoonotic species during the last decade, such as avian and swine. Human isolates with the putative binding profile only circulated from 1968 to 1977, which explains the binding of only HK68/H3 and Vic75/H3 HAs in our H3 panel. In contrast, ~68% of H1 strains (3,016 of 4,462 sequences) possess Lys156, Gly158, and a sterically favorable Ala, Ser, or Thr residue at 193; however, all of these strains also have the 133a insertion that blocks S139/1 binding. In contrast, ~25% of H1 strains (1,120 of 4,462 sequences) do not have the 133a insertion, but of these only six have Lys156 and Gly158, one of which was the A/WSN/1933 (H1N1) (WSN/H1) strain that was included in our binding and neutralization studies.

Although the H13 and H16 strains do not match the putative binding profile, they can also be bound or neutralized by S139/1. One possibility may be because of some plasticity of the receptor binding site as observed from loop insertions in other HA structures (12, 13), where the altered conformations of the loops may alleviate potential clashes with S139/1. Furthermore, the HA1 subdomain positions vary by subtype (13), in comparison with the structurally conserved HA2 stem, and these quaternary variations may also play a role in recognition as in the case of WSN/H1 and A/Adachi/2/1957 (H2N2) that appear to have favorable epitope residues yet bind S139/1 Fab weakly.

1. Yoshida R, et al. (2009) Cross-protective potential of a novel monoclonal antibody directed against antigenic site B of the hemagglutinin of influenza A viruses. *PLoS Pathog* 5:e1000350.
2. Ekiert DC, et al. (2011) A highly conserved neutralizing epitope on group 2 influenza A viruses. *Science* 333:843–850.
3. McCoy AJ, et al. (2007) Phaser crystallographic software. *J Appl Cryst* 40:658–674.
4. Adams PD, et al. (2010) PHENIX: A comprehensive Python-based system for macromolecular structure solution. *Acta Crystallogr D Biol Crystallogr* 66:213–221.
5. McDonald IK, Thornton JM (1994) Satisfying hydrogen bonding potential in proteins. *J Mol Biol* 238:777–793.
6. Sheriff S, Hendrickson WA, Smith JL (1987) Structure of myohemerythrin in the azidomet state at 1.7/1.3 A resolution. *J Mol Biol* 197:273–296.
7. Connolly ML (1983) Analytical molecular surface calculation. *J Appl Cryst* 16:548–558.
8. Abhinandan KR, Martin AC (2008) Analysis and improvements to Kabat and structurally correct numbering of antibody variable domains. *Mol Immunol* 45: 3832–3839.
9. Chen VB, et al. (2010) MolProbity: All-atom structure validation for macromolecular crystallography. *Acta Crystallogr D Biol Crystallogr* 66:12–21.
10. Bao Y, et al. (2008) The influenza virus resource at the National Center for Biotechnology Information. *J Virol* 82:596–601.
11. Edgar RC (2004) MUSCLE: Multiple sequence alignment with high accuracy and high throughput. *Nucleic Acids Res* 32:1792–1797.
12. Xu R, et al. (2010) Structural basis of preexisting immunity to the 2009 H1N1 pandemic influenza virus. *Science* 328:357–360.
13. Russell RJ, et al. (2004) H1 and H7 influenza haemagglutinin structures extend a structural classification of haemagglutinin subtypes. *Virology* 325:287–296.

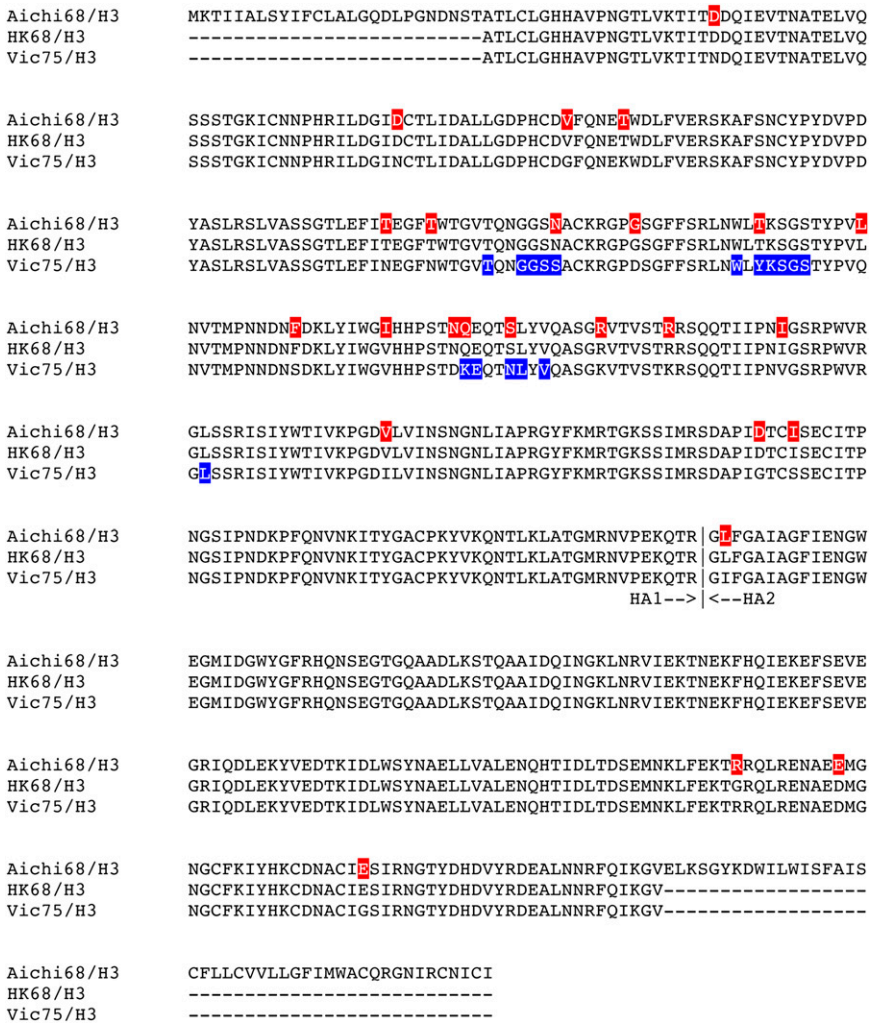

Fig. S1. Sequence alignment of A/Aichi/2/1968 (H3N2) HA versus A/Hong Kong/1/1968 (H3N2) HA and A/Victoria/3/1975 (H3N2) HA strains. Residues in HK68/H3 or Vic75/H3 that differ from Aichi68/H3 are colored in red. S139/1 binding epitope residues of Vic75/H3 are colored in blue.

```
Sweden/4/99/H16      --------------------DKICIGYLSNNSTDTVDTLTENGVPVTSSIDLVETNHTGTY
Sweden/5/99/H16      MVIKVLYFLIVLLSRYSKADKICIGYLSNNATDTVDTLTENGVPVTSSVDLVETNHTGTY

Sweden/4/99/H16      CSLNGVSPIHLGDCSFEGWIVGNPSCASNINIREWSYLIEDPNAPHKLCFPGEVDNNGEL
Sweden/5/99/H16      CSLNGISPIHLGDCSFEGWIVGNPSCATNINIREWSYLIEDPNAPNKLCFPGELDNNGEL

Sweden/4/99/H16      RHLFSGVNSFSRTELIPPSKWGDILEGTTASCQNRGANSFYRNLIWLVNKLN-KYPVVKG
Sweden/5/99/H16      RHLFSGVNSFSRTELISPNKWGDILDGVTASCRDNGASSFYRNLVWLVKNKNGKYPVIKG

Sweden/4/99/H16      EYNNTTGRDVLVLWGIHHPDTEATANKLYVNKNPYTLVSTKEWSRRYELEIGTRIGDGQR
Sweden/5/99/H16      DYNNTTGRDVLVLWGIHHPDTETTATNLYASKNPYTLVSTKEWSKRYELEIGTRIGDGQR

Sweden/4/99/H16      SWMKTYWHLMHPGERITFESSGGLLAPRYGYIIEKYGTGRIFQSGVRLAKCNTKCQTSMG
Sweden/5/99/H16      SWMKLYWHLMRPGERIMFESNGGLIAPRYGYIIEKYGTGRIFQSGVRVAKCNTKCQTSLG

Sweden/4/99/H16      GINTNKTFQNIERNALGDCPKYIKSGQLKLATGLRNVPSIVER|GLFGAIAGFIEGGWPG
Sweden/5/99/H16      GINTNKTFQNIERNALGDCPKYIKSGQLKLATGLRNVPSVGER|GLFGAIAGFIEGGWPG
                                                        HA1-->|<--HA2

Sweden/4/99/H16      LINGWYGFQHQNEQGTGIAADKTSTQKAINEITTKINNIIEKMNGNYDSIRGEFNQVEKR
Sweden/5/99/H16      LINGWYGFQHQNEQGTGIAADKASTQKAIDEITTKINNIIEKMNGNYDSIRGEFNQVEKR

Sweden/4/99/H16      INMIADRVDDAVTDIWSYNAKLLVLIENDRTLDLHDANVRNLHEQIKRALKDNAIDEGDG
Sweden/5/99/H16      INMLADRVDDAVTDIWSYNAKLLVLLENGRTLDLHDANVRNLHDQVKRLLKSNAIDEGDG

Sweden/4/99/H16      CFSILHKCNDSCMETIRNGTYNHEDYREESQLKRQEIEGI--------------------
Sweden/5/99/H16      CFNLLHKCNDSCMETIRNGTYNHEDYREESQLKRQEIEGIKLKSEDNVYKVLSIYSCIAS

Sweden/4/99/H16      ----------------------------
Sweden/5/99/H16      SIVLVGLILAFIMWACSNGNCRFNVCI
```

Fig. S2. Sequence alignment of A/black-headed gull/Sweden/4/1999 (H16N3) HA and A/black-headed gull/Sweden/5/1999 (H16N3) HA. Residues that differ are colored in red.

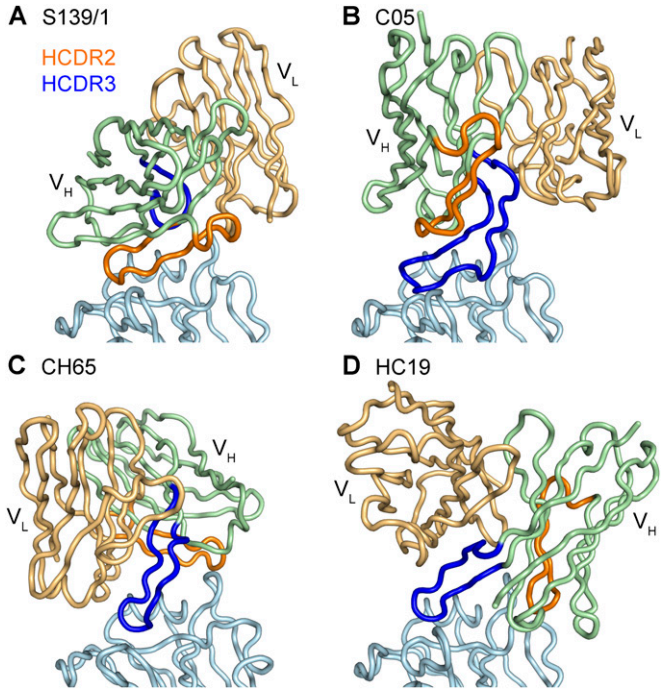

Fig. S3. Comparison of the binding modes of receptor binding site-targeted antibodies S139/1, C05, CH65, and HC19. The orientation of S139/1 and C05 versus HC19 and CH65 on their epitopes in and around the receptor binding site differ by an ~180° rotation on the HA surface. (*A*) S139/1 inserts HCDR2 into the receptor binding site, whereas (*B*) C05 (PDB ID code 4FP8), (*C*) CH65 (PDB ID code 3SM5), and (*D*) HC19 (PDB ID code 2VIR) insert HCDR3 into the receptor binding site. The heavy and light chains of the Fabs are colored green and light orange, respectively, and only the variable domains are shown. HA is colored in light blue.

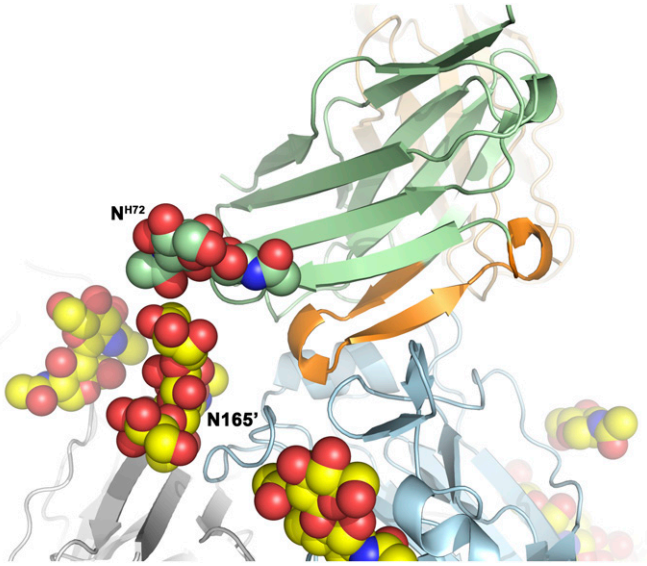

Fig. S4. S139/1 contains an N-linked glycosylation site at Asn72 in the FR3 of the heavy chain that comes into close proximity with the glycan on Asn165 from a neighboring protomer of Vic75/H3 HA. HCDR2 is colored in orange.

```
                <------------FWR1------------>  <CR1>  <-----FWR2--->
S139/1          QVQLQQSGTELKKPGASVKISCKATGYTFS  SYWIE  WIKQRPGHGLEWIG
J558.17         ........A..M.................  .....  .V............

                <------CDR2-----> <--------------FWR3------------>
S139/1          EILPEIGMTNYNENFKG KATFTANTSSNTVYMQLSSLTSEDSAVYYCAR
J558.17         ....GS.S.....K... ......D.....A.................--
```

Fig. S5. Sequence alignment of S139/1 V_H and mouse germ-line J588.17. S139/1 HCDR2 residues that contact HA are colored in red.

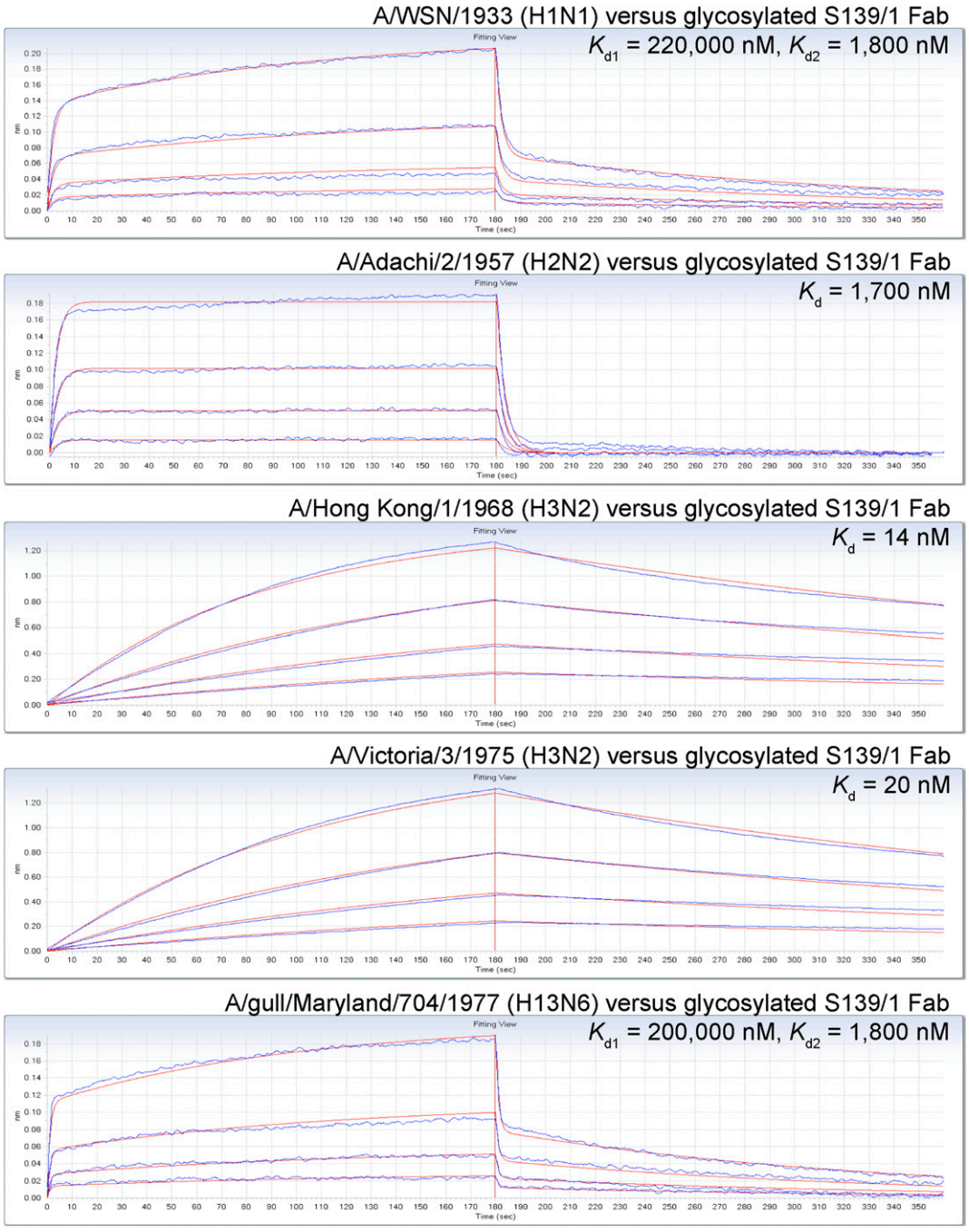

Fig. S6. Binding curves for reported K_d values for glycosylated S139/1 Fab. Blue curves are the experimental trace obtained from bio-layer interferometry experiments and red curves are the best global fits to the data used to calculate the K_d values reported in Table 1.

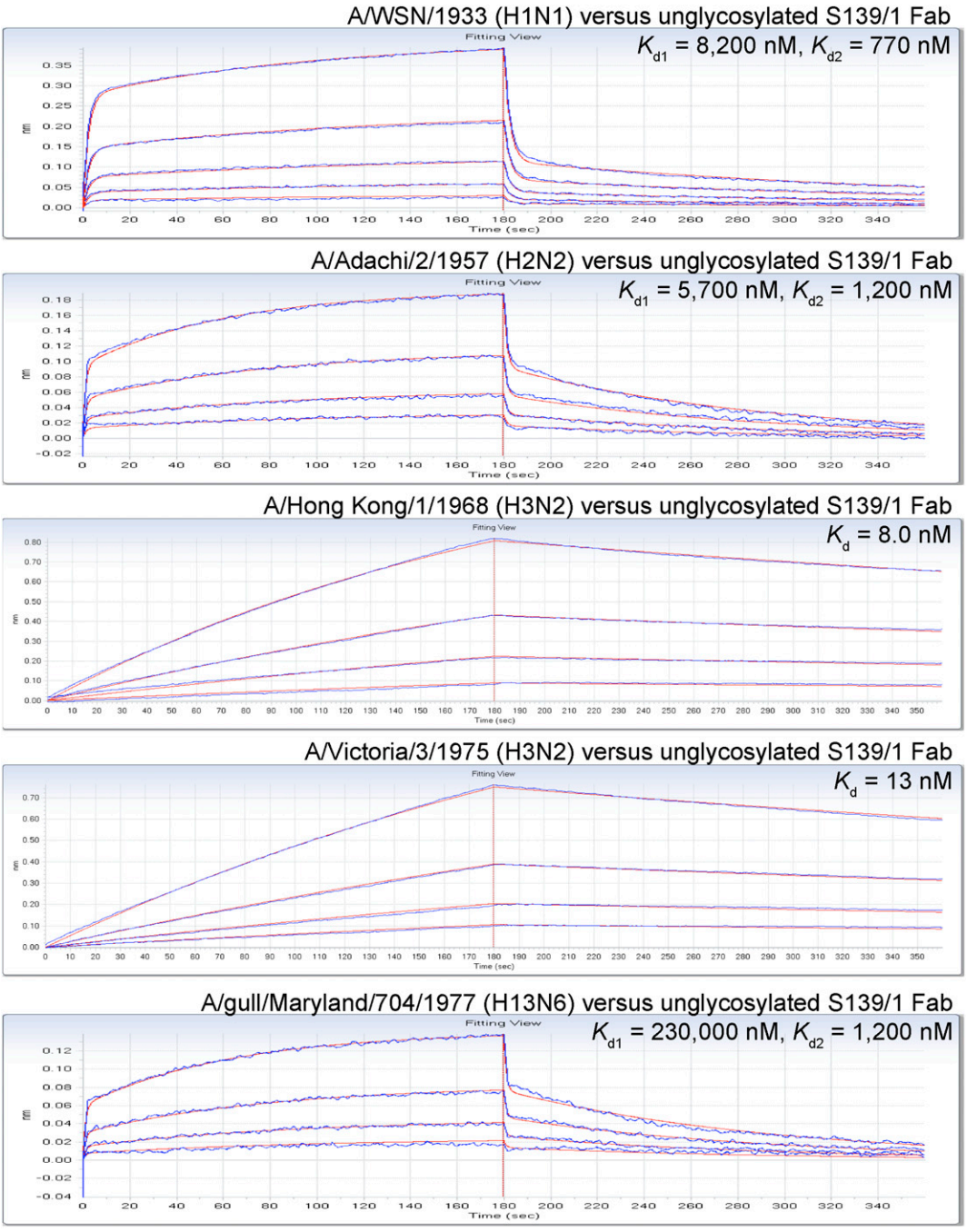

Fig. S7. Binding curves for reported K_d values for unglycosylated S139/1 Fab. Blue curves are the experimental trace obtained from bio-layer interferometry experiments and red curves are the best global fits to the data used to calculate the K_d values reported in Table 1.

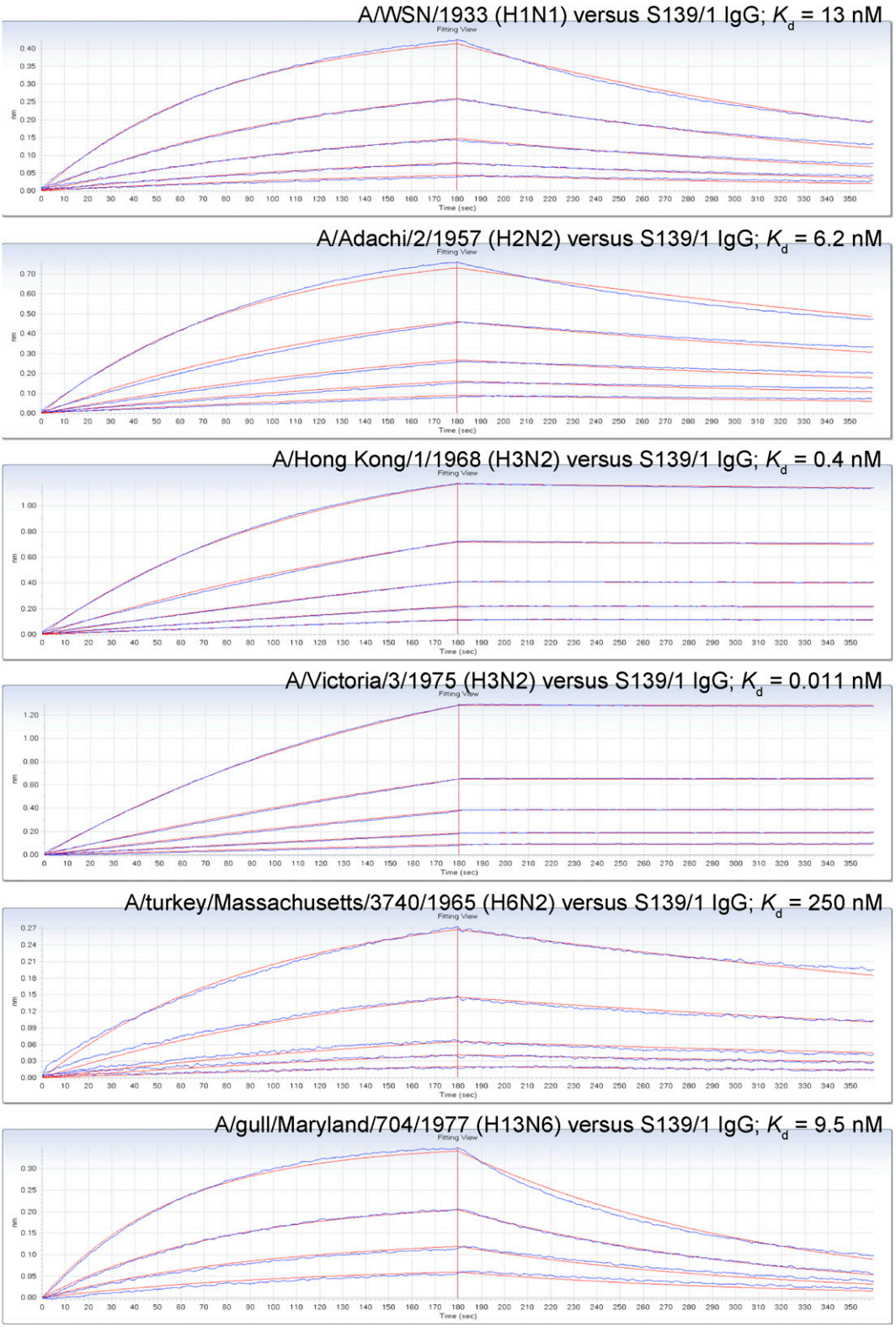

Fig. S8. Binding curves for reported K_d values for S139/1 IgG. Blue curves are the experimental trace obtained from bio-layer interferometry experiments and red curves are the best global fits to the data used to calculate the K_d values reported in Table 1.

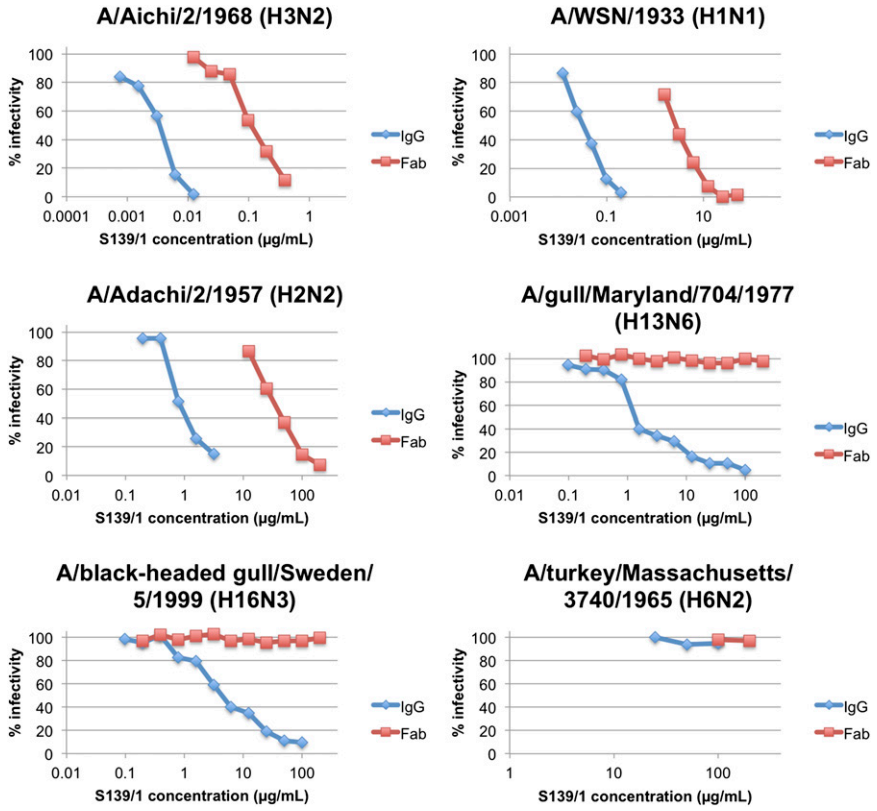

Fig. S9. Neutralization activity of S139/1 evaluated by plaque reduction using Madin-Darby canine kidney cells. IC_{50} values for S139/1 Fab and IgG reported in Table 1.

Table S1. Influenza HA strains tested with no detectable binding by S139/1 Fab and IgG

Isolate	Fab K_d	IgG K_d
A/South Carolina/1/1918 (H1N1)	>1 μM	>10 μM
A/New York/1/1918 (H1N1)	>1 μM	>10 μM
A/Puerto Rico/8/1934 (H1N1)	>1 μM	>10 μM
A/AA/Marton/1943 (H1N1)	>1 μM	>10 μM
A/duck/Alberta/345/1976 (H1N1)	>1 μM	>10 μM
A/USSR/90/1977 (H1N1)	>1 μM	>10 μM
A/Singapore/6/1986 (H1N1)	>1 μM	>10 μM
A/Texas/36/1991 (H1N1)	>1 μM	>10 μM
A/Beijing/262/1995 (H1N1)	>1 μM	>10 μM
A/Solomon Islands/3/2006 (H1N1)	>1 μM	>10 μM
A/California/04/2009 (H1N1)	>1 μM	>10 μM
A/Japan/305/1957 (H2N2)	>1 μM	>10 μM
A/duck/Ukraine/1/1963 (H3N8)	>1 μM	>10 μM
A/Bangkok/1/1979 (H3N2)	>1 μM	>10 μM
A/Beijing/353/1989 (H3N2)	>1 μM	>10 μM
A/Shangdong/9/1993 (H3N2)	>1 μM	>10 μM
A/Panama/2007/1999 (H3N2)	>1 μM	>10 μM
A/Moscow/10/1999 (H3N2)	>1 μM	>10 μM
A/Brisbane/10/2007 (H3N2)	>1 μM	>10 μM
A/Perth/16/2009 (H3N2)	>1 μM	>10 μM
A/duck/Czechoslovakia/1956 (H4N6)	>1 μM	>10 μM
A/Vietnam/1203/2004 (H5N1)	>1 μM	>10 μM
A/Indonesia/05/2005 (H5N1)	>1 μM	>10 μM
A/Netherlands/219/2003 (H7N7)	>1 μM	>10 μM
A/chicken/Germany/N/1949 (H10N7)	>1 μM	>10 μM
A/duck/Alberta/60/1976 (H12N5)	>1 μM	>10 μM
A/mallard duck/Astrakhan/263/1982 (H14N5)	>1 μM	>10 μM
A/shearwater/Western Australia/2576/1979 (H15N8)	>1 μM	>10 μM
A/black-headed gull/Sweden/4/1999 (H16N3)	>1 μM	>10 μM

Table S2. Binding breadth of influenza strains by glycosylated and unglycosylated S139/1 Fab

Isolate	Glycosylated Fab K_d (nM)	Unglycosylated Fab K_d (nM)
A/Hong Kong/1/1968 (H3N2)	14	8
A/Victoria/3/1975 (H3N2)	20	13
A/WSN/1933 (H1N1)	1,800	770
A/Adachi/2/1957 (H2N2)	1,700	1,200
A/gull/Maryland/704/1977 (H13N6)	1,800	1,200

See also Table S4 and *SI Materials and Methods.*

Table S3. HA sequence variation at the S139/1 epitope for strains with no binding activity

Isolate	133a	156	158	150 loop insertion	193
A/Aichi/2/1968 (H3N2) HA used to raise S139/1	–	K	G	No	S
A/South Carolina/1/1918 (H1N1)	K	–	–	–	–
A/New York/1/1918 (H1N1)	K	–	–	–	–
A/Puerto Rico/8/1934 (H1N1)	–	E	E	–	N
A/AA/Marton/1943 (H1N1)	R	E	D	–	T
A/duck/Alberta/345/1976 (H1N1)	K	–	–	–	–
A/USSR/90/1977 (H1N1)	R	E	Nψ	–	T
A/Singapore/6/1986 (H1N1)	K	–	Nψ	–	A
A/Texas/36/1991 (H1N1)	K	E	N	–	A
A/Beijing/262/1995 (H1N1)	–	E	N	–	A
A/Solomon Islands/3/2006 (H1N1)	–	G	N	–	A
A/California/04/2009 (H1N1)	K	–	–	–	–
A/Japan/305/1957 (H2N2)	–	E	–	–	T
A/duck/Ukraine/1/1963 (H3N8)	–	–	E	–	D
A/Bangkok/1/1979 (H3N2)	–	E	E	–	N
A/Beijing/353/1989 (H3N2)	–	E	E	–	N
A/Shangdong/9/1993 (H3N2)	–	–	E	–	–
A/Panama/2007/1999 (H3N2)	–	Q	K	–	–
A/Moscow/10/1999 (H3N2)	–	Q	K	–	–
A/Brisbane/10/2007 (H3N2)	–	H	K	–	F
A/Perth/16/2009 (H3N2)	–	H	N	–	F
A/duck/Czechoslovakia/1956 (H4N6)	–	–	–	Yes	N
A/Vietnam/1203/2004 (H5N1)	L	–	Nψ	–	K
A/Indonesia/05/2005 (H5N1)	S	–	Nψ	–	R
A/Netherlands/219/2003 (H7N7)	–	S	N	Yes	K
A/chicken/Germany/N/1949 (H10N7)	A	–	–	Yes	D
A/duck/Alberta/60/1976 (H12N5)	–	L	S	Yes	K
A/mallard duck/Astrakhan/263/1982 (H14N5)	–	–	N	Yes	D
A/shearwater/Western Australia/2576/1979 (H15N8)	–	S	N	Yes	K
A/black-headed gull/Sweden/4/1999 (H16N3)	–	N	L	–	K

Identical residues in comparison with A/Aichi/2/1968 (H3N2) HA are denoted by a hyphen. Unfavorable residues are boxed in black and tolerable residues are boxed in gray. Nψ indicates an N-linked glycosylation site.

Table S4. Electrospray-ionization–MS analysis of baculovirus expressed and purified S139/1 Fab

	Expected mass (Da)	ESI-MS mass (Da)
S139/1 Fab	48,277	
Purified glycosylated S139/1 Fab		49,437
Purified monoglycosylated S139/1 Fab		48,456
Purified unglycosylated S139/1 Fab		48,253

ESI-MS, electrospray ionization–mass spectrometry.

Other Supporting Information Files

Dataset S1 (DOCX)